

# Proceedings of the ASME National Heat Transfer Conference, Baltimore, August, 1997.

## EVAPORATION OF A SMALL WATER DROPLET CONTAINING AN ADDITIVE

Michelle D. King, Jiann C. Yang<sup>1</sup>, Wendy S. Chien, and William L. Grosshandler

Building and Fire Research Laboratory  
National Institute of Standards and Technology  
Gaithersburg, Maryland 20899, U.S.A.

### ABSTRACT

An experimental study on the evaporation of a small water droplet containing an additive on a heated, polished stainless-steel surface was performed. Solutions of water containing 30 % (w/w) and 60 % (w/w) of potassium acetate and sodium iodide were used in the experiments. Surface temperatures used in the experiments ranged from 50 °C to 100 °C. The average evaporation rates for the potassium acetate and sodium iodide solutions were found to be lower than that of pure water at a given surface temperature. A simple evaporation model was developed to interpret the experimental results.

### INTRODUCTION

Fine water systems have several advantages over conventional fire protection sprinklers in certain applications when water supply is limited and collateral damage by water is a concern. These systems have recently been considered as a potential replacement for halon fire-protection systems in shipboard machinery spaces and crew compartments of armored vehicles. However, below 0 °C water will freeze, thus posing a limitation in low temperature operations. Certain additives, if selected properly, not only can suppress the freezing point of water but also can improve its fire suppression effectiveness. Some water-based agents have recently been proven to be more effective than pure water when applied in the form of mist to suppress a small jet fuel pool fire (Finnerty *et al.*, 1996). Among the thirteen agents tested, potassium lactate (60% w/w), potassium acetate (60% w/w), and sodium bromide (10% w/w) were found to be superior as fire-extinguishing sprays than pure water and other candidate solutions. The suppression benefit of adding a solute to a water spray was only noted when the spray was applied directly toward the fire; however, the effect of these additives on the overall fire suppression effectiveness when the spray is not directed toward the base of the fire remains unclear.

When a fine mist is formed in a nozzle, the majority of the droplets are unlikely to penetrate to the base of the fire because the droplet momentum

is small enough that they are deflected away by the rising plume (Downie *et al.*, 1995). The deflected mist droplets subsequently experience a cooler environment outside the hot gas plume, thus resulting in slow droplet evaporation. Some of the slowly vaporizing droplets will impinge upon the enclosure surfaces wherein the fire is located, or upon obstacles within the enclosure. These droplets will eventually be vaporized on the heated surfaces. Droplets that impinge on these surfaces in the vicinity of the fire zones can still play many indirect roles in facilitating fire suppression through (1) surface cooling, thus mitigating flame spread and (2) entrainment of water vapor from the evaporating droplets into the flame. Therefore, rapid evaporation of water droplets from the surrounding heated surfaces may be desirable. The evaporation of water/additive droplets may not be an important issue if the droplets can penetrate the hot plume and reach the base of the fire. However, the role of the deflected droplets and their subsequent evaporation becomes significant if only a small amount of droplets with significant momentum can penetrate the flame.

While the addition of a solute to water may improve the suppression effectiveness within the fire through chemical or physical means, it may also affect the droplet vaporization and generation processes. The addition of a solute lowers vapor pressure and the mass transfer driving force for evaporation, elevates the boiling point of the solvent, and modifies other physical properties of water. Furthermore, the addition of solute decreases the relative amount of water in a droplet (e.g., 60% w/w potassium lactate solution). For droplets that fall outside the flame zone, the solid residuals of the solute are left deposited on the heated surface after the water has been evaporated and may not contribute to the chemical suppression process.

The evaporation of suspended droplets containing dissolved solids in a hot ambience was first studied by Charlesworth and Marshall (1960). The formation of a solid crust and various appearance changes during the course of evaporation under a wide range of experimental conditions were observed. Three major evaporation stages were identified: (1) evaporation before the formation of the solid phase, (2) progressive formation of the solid phase about the droplet, and (3) evaporation during the solid phase

<sup>1</sup>Author to whom correspondence should be addressed.

formation. Several studies on droplets with dissolved solids have since been conducted (see *e.g.*, Nešić and Vodnik, 1991; Kudra *et al.*, 1991; Taniguchi and Asano, 1994). The formation of dried solids in a droplet impedes the evaporation process of the droplet. Liquid in the interior of the droplet must reach the surface in order to evaporate. Increasing the amount of solute increases the resistance to mass transfer inside the droplet, slowing the movement of moisture out of the droplet (Masters, 1985). However, to the best of our knowledge, no research has been performed on the evaporation of a water droplet with a dissolved salt on a heated surface.

The objective of the present work is to examine the evaporation characteristics of some water-based fire suppressing agents on a heated surface at temperatures below nucleate boiling. Because of its potentially superior fire suppression ability and its use in suppressing cooking grease fires, water with dissolved potassium acetate was used in the experiments. Sodium iodide was selected as another additive in lieu of sodium bromide (recommended by Finnerty *et al.*, 1996) because it is believed that the iodine compound may be more effective in fire suppression than its bromine counterpart (Pitts *et al.*, 1990). Previous studies (*e.g.*, diMarzo and Evans, 1989; Chandra and Avedisian, 1991; Qiao and Chandra, 1996) were focused on relatively large drops (above 1 mm in diameter) of pure solvents (water or hydrocarbons) or water with a small amount of surfactant added. For the present work, smaller droplets of highly concentrated electrolyte solutions with diameters between 0.3 mm and 0.6 mm (to simulate mist droplets) were used.

## EXPERIMENTAL METHOD

Figure 1 shows a schematic diagram of the experimental apparatus. It consists of a droplet generator, a solution reservoir, a nickel-plated copper block equipped with two small cartridge heaters, a stainless steel surface, a temperature controller, and a CCD camera. The droplet generator has a chamber, a piezoelectric ceramic disc, and a glass nozzle (Yang *et al.*, 1997) and is based on the drop-on-demand ink-jet technique. A small droplet is ejected from the nozzle as a result of the deflection of the piezoelectric ceramic disc upon application of a squared pulse with controlled amplitude and duration to the disc. The use of this droplet generator enables the production of smaller droplets and repeatable operation. The surface on which the droplet is vaporized is a 5 cm x 3 cm x 0.5 cm polished stainless steel (SS 304) block fastened to the nickel-plated copper block. The 5 cm x 3 cm x 1.25 cm nickel-plated copper block is used to heat the surface to the desired temperature (between 50 °C and 100 °C). Surface temperature is maintained within  $\pm 1$  °C by using a temperature controller. The CCD camera is used to record the evaporation histories of the droplets. The evaporation times (see discussion below) of the droplets can be determined by using frame-by-frame analysis of the video records. The basic experimental procedure involved triggering the generator to deliver a single droplet from the nozzle to the heated surface located 6.5 cm below.

Single-shot stroboscopic photography (see *e.g.*, Chandra and Avedisian, 1991) was used to record the droplet formation at the nozzle exit of the droplet generator, droplet diameters before impact, and average droplet impact velocities. A 35 mm SLR camera equipped with a 105 mm lens and extended bellows, an electronic strobe for backlighting, and an electronic delay timer were used. The average impact velocity, which was taken to be the time between the instant when an electronic pulse was sent to the droplet generator and the instant when the droplet impacted the surface, was found to be 72 cm/s  $\pm$  2 cm/s. No shattering of droplets due to impact on the surface was observed within the range of surface temperatures tested. The Weber number ( $We = \rho_l V^2 D / \sigma$ ) of the droplets was less than 80.

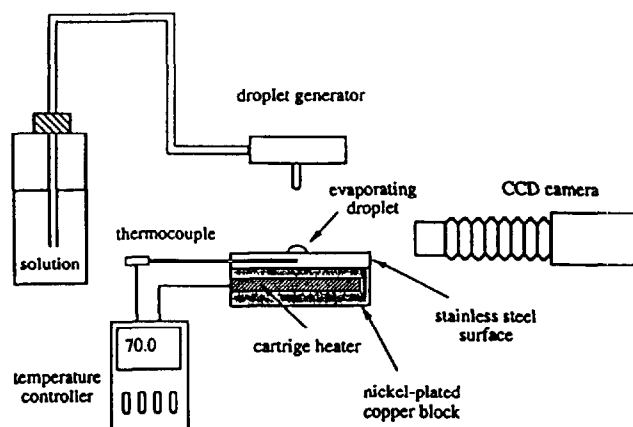


Figure 1. Schematic diagram of experimental apparatus

Since the mass loss of the evaporating droplet in the present experiment was not monitored continuously, it was not possible to determine the time for *complete* evaporation of water from the water/dissolved-solid droplet on the heated surface from the video records because of subsequent formation of solid residual. Therefore, an *apparent* evaporation time of a water droplet with dissolved solid is defined as the time when the solid residual first appears during evaporation with the assumption that the amount of water vaporized before solid formation constitutes the bulk of the initial water content. Such an assumption appears to be reasonable for small droplets with  $D_0 < 1.3$  mm (Charlesworth and Marshall, 1960). The average water evaporation rate is defined as the initial amount of water in the droplet divided by the apparent evaporation time. Knowing the initial solution density, droplet diameter, and solute concentration, the initial mass of water in the droplet can be determined.

Table 1 summarizes the physical properties of the aqueous solutions studied. The surface tensions of the aqueous solutions were determined by using a tensiometer which measured the force required to withdraw a platinum-iridium ring from the surface of the liquid. The surface tensions of sodium iodide solutions are greater than that of distilled water and increase as the concentration increases. For the potassium acetate solutions, it is interesting to note that the 30 % w/w and the 60 % w/w have surface tensions greater than and less than that of pure water, respectively. The densities of the solutions were taken from Söhnel and Novotný (1985), and the solution viscosities and normal freezing points were obtained from Washburn (1929).

## RESULTS AND DISCUSSION

Since droplet formation depends on the initial salt concentration, the resulting initial droplet diameters will differ somewhat. In addition, the initial mass of water in the droplet decreases as the concentration of the dissolved salt increases. For the purpose of comparison, it is more meaningful to plot apparent or average mass evaporation rate than evaporation time as a function of surface temperature. The experimental average water mass evaporation rates at different surface temperatures for 0 %, 30 %, and 60 % potassium acetate and sodium iodide solutions are shown in Figure 2. The error bars in the figures are the 2- $\sigma$  (standard deviation) of at least six runs. The large scatter in some of the experimental data reflects the difficulty in determining the first appearance of solid

Table 1. Physical properties of the solutions

Fluid	Density @ 22 °C (g cm <sup>-3</sup> )	Viscosity (g s <sup>-1</sup> cm <sup>-1</sup> ) x 10 <sup>3</sup>	Normal Freezing point (°C)	Surface tension (@ 22 °C) (dyne cm <sup>-1</sup> ) ± 2 dyne cm <sup>-1</sup>
Distilled water	1.00	9.6 (@ 22 °C)	0	72
30% potassium acetate	1.16	22.8 (@ 18 °C)	-23	73
60% potassium acetate	1.34	50.9 (@ 18 °C)	— <sup>a</sup>	68
30% sodium iodide	1.29	10.9 (@ 20 °C)	-18	76
60% sodium iodide	1.80	23.4 (@ 20 °C)	— <sup>a</sup>	78

<sup>a</sup>Not available from literature

formation. The addition of potassium acetate or sodium iodide to water decreases the evaporation rate below that of pure water as shown in the figure. As the concentration of dissolved salt increases, the average evaporation rate becomes slower.

### Heat and Mass Transfer Analysis

A simple model for predicting the average evaporation rate of a water droplet containing a dissolved solid on a heated surface is formulated in an attempt to compare with the experimental observations. The problem description is as follows. A droplet impinges on the heated surface and spreads. The spread droplet then evaporates due to heat transfer from the heated surface. The droplet evaporation model is based on the following simplifying description of the process:

1. After impact on the heated surface, the droplet immediately assumes the shape of a truncated sphere, whose diameter of the contact circle with the surface is taken to be the maximum spread diameter of the droplet, as shown in Figure 3.
2. The time for the droplet to attain its maximum spread diameter is negligible compared to the droplet evaporation time on the heated surface.
3. The droplet maintains its initial maximum spread diameter during evaporation; therefore, only  $H$  is a function of time (see Figure 3).
4. The heated surface is treated as an infinite thermal reservoir.
5. Molecular diffusion dominates at the vapor-liquid interface.
6. The instantaneous concentration of the dissolved solid in the droplet is spatially uniform during evaporation, and liquid-vapor phase equilibrium is maintained at the droplet surface.

The calculated evaporation time is defined as the time between impact and when the dissolved solute mole fraction,  $X_d(t)$ , becomes equal to the solubility of the solute,  $X_{d,sat}(t)$ ; i.e., a phase transition from dissolved solute to a solid phase will occur when  $X_d(t) = X_{d,sat}(t)$ . Note that the solubility of the solute is a function of time because the droplet temperature is changing.

After the droplet has impinged on the surface, its maximum spread diameter can be estimated by using the following empirical correlation

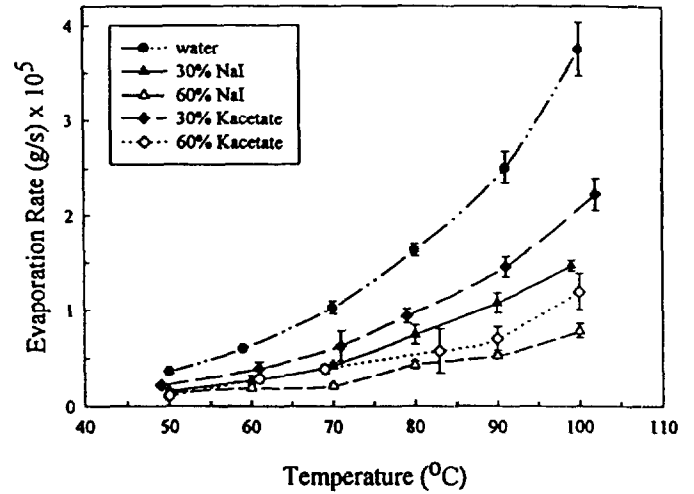


Figure 2. Experimental average mass evaporation rates at different surface temperatures

(Scheller and Bousfield, 1995):

$$\frac{D_{max}}{D_o} = 0.61 (Re \sqrt{We})^{0.166} \quad (1)$$

where the Reynolds number  $Re$  is based on the initial droplet diameter before impact. The assumption of maximum spread is reasonable because it was observed in this study that during most of the evaporation period the contact diameter between a water droplet containing a dissolved salt and the heated surface remained relatively constant. The spread diameter is required for the calculation of heat transfer from the heated surface to the droplet. The instantaneous droplet height  $H$  of the spherical segment can be calculated by equating the mass of the initial droplet (before impact) to that of the truncated sphere.

$$\frac{1}{6} \pi H \left( \frac{3}{4} D_{max}^2 + H^2 \right) = \frac{\pi}{6} D_o^3 \quad (2)$$

Once  $H$  is determined, the radius of curvature  $R_c$  of the truncated sphere can be obtained by the following equation (Beyer, 1981):

$$R_c = \frac{1}{6H} \left( \frac{3}{4} D_{max}^2 + H^2 \right) + \frac{H}{3} \quad (3)$$

The instantaneous heat transfer rate from the heated surface to the droplet is approximated by

$$\dot{Q} \approx A_s \frac{k_l (T_w - T_s)}{\delta} \quad (4)$$

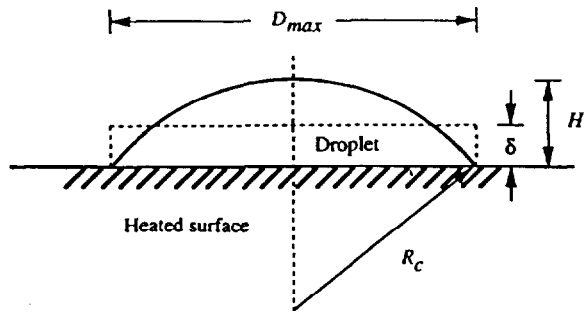


Figure 3. Droplet-geometry for heat and mass transfer analysis

In writing Equation (4), the heat transfer is modeled as a thin right circular cylinder with a thickness  $\delta$  (see Figure 3) and an equivalent volume equal to the spherical segment, and the temperature profile within the droplet is assumed to be linear (Bonacina *et al.*, 1979). If the heat transferred to the droplet from the surface is used solely to evaporate the liquid from the liquid-vapor interface, then an energy balance on the evaporating droplet can be expressed as

$$\dot{m} \Delta H_v = \dot{Q} \quad (5)$$

Following the treatment given in Bird *et al.* (1960), the instantaneous evaporation rate can be written as

$$\dot{m} = k_m A_f \ln \left[ 1 + \frac{Y_{ws} - Y_{\infty}}{1 - Y_{ws}} \right] \quad (6)$$

In order to calculate the evaporation rate  $\dot{m}$ , the value of  $T_s$  or  $Y_{ws}$  is needed. Using Equations (4), (5), and (6), one gets

$$k_m A_f \ln \left[ 1 + \frac{Y_{ws} - Y_{\infty}}{1 - Y_{ws}} \right] = A_b \frac{k_f (T_w - T_s)}{\delta \Delta H_v} \quad (7)$$

If equilibrium is assumed at the liquid-vapor interface and the vapor phase is assumed to be an ideal gas mixture, then equating the component fugacities in both phases (Prausnitz *et al.*, 1986) results in

$$Y_{ws} \approx \frac{P_{solution}}{P_i} \quad (8)$$

where  $P_{solution}$  is the vapor pressure of the aqueous solution. The reduction of vapor pressure due to the presence of the dissolved solid can be seen in Equation (8) since without the dissolved solid,  $P_{solution}$  equals to  $P_{w,sat}$ , assuming the solubility of air in water is negligible under atmospheric conditions. Knowing the vapor pressure of the solution to be a function of droplet surface temperature, Equation (7) can be solved for  $T_s$ . Once  $T_s$  is known, the evaporation rate  $\dot{m}$  can be calculated by using Equations (4) and (5).

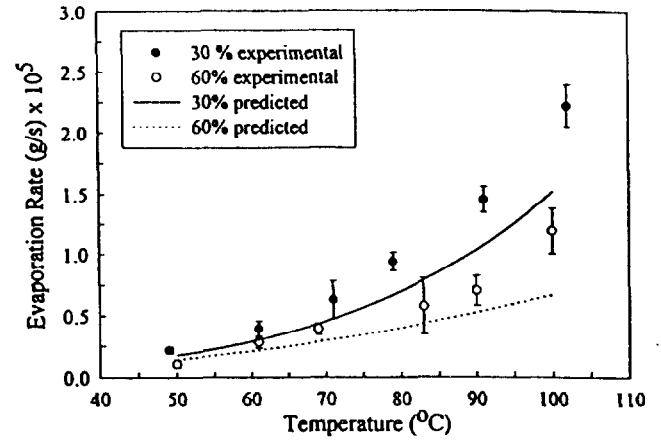


Figure 4. Experimental and predicted average evaporation rates of potassium acetate at various surface temperatures

Since mass transfer coefficients of spherical droplets are readily available in the literature, the mass transfer process is treated as if the truncated droplet were evaporating as a spherical droplet with a radius equivalent to the radius of curvature  $R_c$  of the truncated sphere. In this case, the mass transfer coefficient  $k_m$  can then be estimated by using the Chilton-Colburn analogy (Bird *et al.*, 1960).

$$\frac{k_m 2R_c}{c_f D_{wsf}} = 2 \quad (9)$$

Calculations were performed for two different concentrations of potassium acetate and sodium iodide solutions (see the Appendix for calculation procedure). Figures 4 and 5 compare the predicted and measured average evaporation rates of the two aqueous solutions at different surface temperatures. The predicted values were obtained based on the average initial droplet diameters used in all the experiments with the same initial dissolved salt concentration. Since most of the estimation methods for the physical properties of aqueous electrolyte solutions are primarily applicable to dilute or moderately concentrated solutions at 25°C, a certain degree of extrapolation had to be used in the calculations for concentrated solutions at higher temperatures when no literature values were available. The discrepancies between the predictions and measurements in Figures 4 and 5 may be largely attributed to the estimation methods. However, the disagreements are equally likely due to the simplified heat and mass transfer models used in the analysis and the time-averaging of the evaporation rate.

Direct comparison of the results between the two aqueous solutions with the same initial salt concentration proves to be not straightforward. The degree of vapor pressure lowering due to the presence of a salt depends on the ionic strength of the solution. The two aqueous solutions used in the experiments are not at the same ionic strength despite the same initial mass fraction of salt in the solutions. Even if solutions with same ionic strength and same initial droplet diameters were used, the spread of the liquid droplet after impact would still differ because of different Reynolds and Weber numbers. This would change the heat and mass transfer processes between the droplet and the surface. Therefore, it is difficult to interpret the results

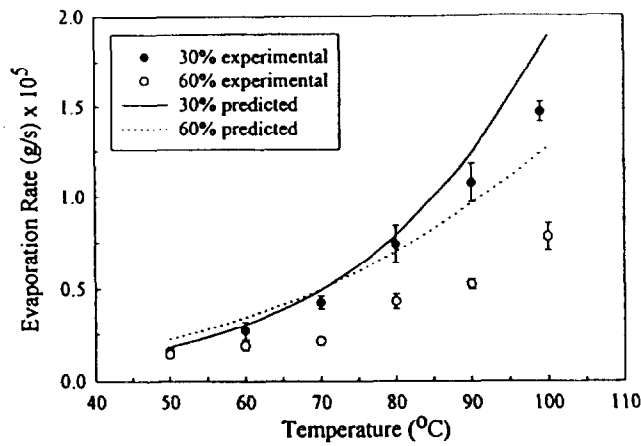


Figure 5. Experimental and predicted average mass evaporation rates of sodium iodide at various surface temperatures

in Figures 4 and 5 solely based on the effect of vapor pressure lowering on the evaporation rate, although for solutions with the same ionic strength, the degree of vapor pressure lowering at a given temperature is less for potassium acetate than for sodium iodide (Washburn, 1929).

The evaporation model described above is rudimentary compared to those previously developed for pure water evaporation (e.g., DiMarzo and Evans, 1989; Qiao and Chandra, 1997); however, the model does not require *a priori* information (i.e., convective heat transfer correlations or spread diameter and contact angle measurements) other than initial droplet diameters, droplet impact velocities, and initial physical properties of the solutions. Since the heat transfer rates to the droplets were directly or indirectly measured and used as input in their analysis, it is not surprising that the models developed by DiMarzo and Evans (1989) and Qiao and Chandra (1997) correlate the experimental data very well. However, the present model overpredicts the evaporation times of pure water. This is probably partially due to the simplified heat transfer model and partially due to the breakdown of Equation (9) in the mass transfer analysis. Since the mass transfer coefficient depends on the radius of the curvature in Equation (9), it will approach zero as  $R_c \rightarrow \infty$ . As the droplet is evaporating,  $R_c$  is increasing as a result of decreasing  $H$ , and the instantaneous mass evaporation rate is asymptotically approaching zero at later times, thus resulting in a relatively long droplet evaporation lifetime. If the average mass evaporation rate of pure water were calculated based on a final mass of 20 % (rather than 0 %) water remaining in order to circumvent this asymptotical behavior, the calculated evaporation rates would correlate well with the measurements. This situation is not encountered in the calculation for a droplet with a dissolved salt because the solute concentration reaches its saturation value before  $H$  is significantly reduced.

## CONCLUSIONS

Experiments on the evaporation of a small droplet with a dissolved salt on a heated surface have been performed as part of an assessment of the performance of water with an additive as a fire suppressant. The surface temperatures varied from 50 °C to 100 °C. Two salts, potassium acetate and sodium iodide, were used. The addition of potassium acetate and sodium iodide decreases the average evaporation rates. At a given surface temperature, the average mass evaporation rate decreases as the

concentration of the dissolved salt increases. A simple evaporation model was developed. Despite the assumptions, idealization, and the uncertainties associated with the thermophysical property estimations of the concentrated electrolyte solutions, this simple analysis captures most of the essential characteristics of the evaporation process of a droplet with a dissolved solid on a heated surface and agrees qualitatively with the trend of the experimental data.

Several issues regarding the application of dissolved salts in water in fire suppression should be carefully considered. If the aqueous solution droplets penetrate the fire plume and reach the fire, the chemical suppression action of the salt could be fully utilized, and the reduction in water evaporation rate due to the added salt would not be a governing factor. On the other hand, if most of the droplets were deflected away from the fire, the chemical suppression effectiveness of the salt would be minimized or lost, and the reduction in water evaporation rate would impose an additional penalty because for a given time less water vapor would be generated and entrained into the adjacent fire for suppression.

## ACKNOWLEDGMENTS

The authors would like to thank Professors. S. Chandra of the University of Toronto and S. C. Yao of Carnegie-Mellon University for many helpful suggestions and discussions.

## NOMENCLATURE

- $A_b$  = contact surface area of the truncated sphere =  $\pi D_{max}^2/4$ , cm<sup>2</sup>
- $A_f$  = droplet free surface area =  $2\pi R_c H$ , cm<sup>2</sup>
- $c$  = vapor concentration, mole/cm<sup>3</sup>
- $D_{max}$  = maximum spread diameter of the droplet after impact, cm
- $D_o$  = initial droplet diameter (before impact), cm
- $D_{wa}$  = diffusion coefficient of water vapor in air, cm<sup>2</sup>/s
- $H$  = height of the truncated sphere, cm
- $\Delta H_v$  = latent heat of vaporization of water, J/mole
- $k_l$  = thermal conductivity of the liquid, J/cm s K
- $k_m$  = mass transfer coefficient, mole/ s cm<sup>2</sup>
- $m_i$  = mass transfer rate, mole/s
- $P$  = pressure, dyne/cm<sup>2</sup>
- $\dot{Q}$  = heat transfer rate, J/s
- $R_c$  = radius of curvature of the truncated sphere, cm
- $Re$  = Reynolds number =  $\rho_l D_o V/\mu_l$
- $T$  = temperature, K
- $T_w$  = temperature of the heated surface, K
- $V$  = impact velocity of the droplet, cm/s
- $We$  = Weber number =  $(\rho_l V^2 D_o/\sigma)$
- $X$  = mole fraction in the liquid phase
- $Y$  = mole fraction in the vapor phase
- $\delta$  = equivalent heat conduction distance, cm
- $\mu$  = viscosity, g/cm s
- $\rho$  = density, g/cm<sup>3</sup>
- $\sigma$  = surface tension of the liquid, dyne/cm
- $\Delta\tau$  = time step, s

## Subscripts

- $d$  = dissolved solid
- $f$  = at film temperature [=  $(T_w + T_\infty)/2$ ] or at film mole fraction  
[ =  $(Y_{w_i} + Y_{w_\infty})/2$ ]

$l$  = liquid phase  
 $o$  = initial  
 $s$  = droplet surface  
 $t$  = total  
 $sat$  = saturation  
 $w$  = water or heated surface  
 $\infty$  = ambience

## REFERENCES

- Beyer, W. H., *CRC Standard Mathematical Tables*, 27th ed., CRC Press, Boca Raton, 1981.
- Bird, R. B., Stewart, W. E., and Lightfoot, E. N., *Transport Phenomena*, John Wiley & Sons, New York, 1960.
- Bonacina, C., Del Giudice, S., and Comini, G., "Dropwise Evaporation," *ASME Journal of Heat Transfer*, Vol. 101, August 1979, pp. 441-446.
- Chandra, S., and Avedisian, C. T., "On the Collision of a Droplet with a Solid Surface," *Proceedings of the Royal Society of London A*, Vol. 432, 1991, pp. 13-41.
- Charlesworth, D. H., and Marshall, W. R., Jr., "Evaporation from Drops Containing Dissolved Solids," *A.I.Ch.E. Journal*, Vol. 6, No. 1, March 1960, pp. 9-23.
- Cisternas, L. A., and Lam, E. J., "An Analytic Correlation of Vapour Pressure of Aqueous and Non-Aqueous Solutions of Single and Mixed Electrolytes," *Fluid Phase Equilibria*, Vol. 53, 1989, pp. 243-249.
- Cisternas, L. A., and Lam, E. J., "An Analytic Correlation of Vapour Pressure of Aqueous and Non-Aqueous Solutions of Single and Mixed Electrolytes. Part II. Application and Extension," *Fluid Phase Equilibria*, Vol. 62, 1991, pp. 11-27.
- Daubert, T. E., and Danner, R. P., *Physical and Thermodynamic Properties of Pure Chemicals. Data Compilation*, Hemisphere, New York, 1992.
- Dean, J. A. (editor), *Lange's Handbook of Chemistry*, 12th ed., McGraw-Hill, New York, 1979.
- Downie, B., Polymeropoulos, C., and Gogos, G., "Interaction of a Water Mist with a Buoyant Methane Diffusion Flame," *Fire Safety Journal*, Vol. 24, 1995, pp. 359-381.
- Finnerty, A. E., McGill, R. L., and Slack, W. A., "Water-Based Halon Replacement Sprays," ARL-TR-1138, U.S. Army Research Laboratory, Aberdeen Proving Ground, July 1996.
- Horvath, A. L., *Handbook of Aqueous Electrolyte Solutions, Physical Properties, Estimation and Correlation Methods*, Ellis Horwood Ltd., Chichester, 1985.
- Kudra, T., Pan, Y. K., and Mujumdar, A. S., "Evaporation from Single Droplets Impinging on Heated Surfaces," *Drying Technology*, Vol. 9, No. 3, 1991, pp. 693-707.
- diMarzo, M., and Evans, D. D., "Evaporation of a Water Droplet Deposited on a Hot High Thermal Conductivity Surface," *ASME Journal of Heat Transfer*, Vol. 111, February 1989, pp. 210-213.
- Masters, K., *Spray Drying Handbook*, 4th ed., CRC Press, Boca Raton, 1985.
- Nešić, S., and Vodnik, J., "Kinetics of Droplet Evaporation," *Chemical Engineering Science*, Vol. 46, No. 2, 1991, pp. 527-537.
- Pitts, W. M., Nyden, M. R., Gann, R. G., Mallard, W. G., and Tsang, W., *Construction of an Exploratory List of Chemicals to Initiate the Search for Halon Alternatives*, NIST Technical Note 1279, U. S. Department of Commerce, Washington D.C., August 1990.
- Prausnitz, J. M., Lichtenthaler, R. N., and Gomes de Azevedo, E., *Molecular Thermodynamics of Fluid-Phase Equilibria*, 2nd ed., Prentice-Hall, Englewood Cliffs, 1986.
- Qiao, Y. M., and Chandra, S., "Experiments on Adding a Surfactant to Water Droplets Boiling on a Hot Surface," to be published in *Proceedings of the Royal Society of London A*, 1997.
- Reid, R. C., Prausnitz, J. M., and Poling, B. E., *The Properties of Gases and Liquids*, 4th ed., McGraw-Hill, New York, 1987.
- Scheller, B. L., and Bousfield, D. W., "Newtonian Drop Impact with a Solid Surface," *A.I.Ch.E. Journal*, Vol. 41, No. 6, June 1995, pp. 1357-1367.
- Söhnel, O., and Novotný, P., *Densities of Aqueous Solutions of Inorganic Substances*, Elsevier, Amsterdam, 1985.
- Taniguchi, I., and Asano, K., "Evaporation of an Aqueous Salt-Solution Drop in Dry Air During Crystallization of Salt," *Proceedings of the Sixth International Conference on Liquid Atomization and Spray Systems*, July 18-22, 1994, Palais des Congrès, Rouen, France, pp. 859-866.
- Washburn, E. W. (editor-in-chief), *International Critical Tables of Numerical Data, Physics, Chemistry and Technology*, Vol. 5, 1st ed., McGraw-Hill, New York, 1929.
- Yang, J. C., Chien W., King, M. D., and Grosshandler, W. L., "A Simple Piezoelectric Droplet Generator," submitted to *Experiments in Fluids*, 1997.

## APPENDIX

This appendix describes the procedure to calculate the evaporation time and the average evaporation rate of a droplet with dissolved solid on a heated surface. For given  $D_o$ ,  $V$ ,  $\mu_f$ ,  $\sigma$ , and  $\Delta\tau$ , the following computational scheme may be used:

1. Calculate  $D_{max}$  using Equation (1).
2. Solve for  $H$  and  $R_c$  using Equations (2) and (3) respectively.
3. Calculate  $k_f$  using  $X_w$  and  $(T_s + T_w)/2$ .
4. Calculate  $c_f$  and  $D_{w,f}$  using  $(T_s + T_w)/2$ .
5. Calculate  $k_f^m$  using Equation (9).
6. Calculate  $T_s^m$  using Equations (7) and (8) by iteration.
7. Calculate  $m$  using Equation (5).
8. Calculate the amount of water evaporated ( $\Delta m$ ) during  $\Delta\tau$  which is equal to  $\dot{m} \Delta\tau$ .
9. Calculate new  $X_w$  and  $X_d$ .
10. If  $X_d \approx X_{d,sat}$ , then stop; else calculate  $\rho_f$ , go to Step 2 to recalculate  $H$  and  $R_c$  knowing that  $\Delta m$  has been evaporated over a period of  $\Delta\tau$ , and repeat Steps 3 to 10.

The calculated evaporation time is then the sum of  $\Delta\tau$ 's required to reach  $X_{d,sat}$ , and the average evaporation rate is the ratio of the difference between the initial water content and the final water content at  $X_{d,sat}$  to the total  $\Delta\tau$ s. A time-step  $\Delta\tau$  of 0.1 s was found to be adequate and was used in all the calculations.

The method of Riedel (Horvath, 1985) is used to estimate the thermal conductivity of the solution. The solution density is estimated by the method of Koptev (Horvath, 1985), and the data on  $X_{d,sat}$  are obtained from Dean (1979). The latent heat of vaporization of water as a function of temperature is obtained from Daubert and Danner (1992). Strictly speaking, the latent heat of vaporization of the solution should be used. The vapor pressures of the aqueous solutions are calculated by the method of Cisternas and Lam (1989, 1991). The diffusion coefficient of water vapor in air is estimated by using the method of Fuller *et al.* (Reid *et al.*, 1987), and the vapor concentration  $c_f$  is calculated by assuming the vapor mixture (at film temperature  $T_f$  and  $P$ ) to be ideal.